17. Examination of rosettes subjected to FISH with whole chromosome painting probes revealed that individual chromosome domains are too wide for the structure of the rosette to be in the form of a monolayer. Measurements of the territorial widths of chromosomes 7 and 16 allow for only 16 to 20 chromosomes to complete the full circle of the rosette as a monolayer, suggesting that the arrangement of chromosomes within rosettes is either multilayered or pseudo-multilayered (staggered). In either instance, the packing strategy is likely to introduce variability in the measured spatial separation of chromosomes. Analysis of the three-dimensional arrangement of chromosomes and their centromeric subdomains at the hub of the rosette by confocal or serial-section electron microscopy should clarify this issue.
18. M. Jordan, D. Thrower, L. Wilson, *J. Cell Sci.* **102**, 401 (1992).
19. In rosettes not included in this study because they did not satisfy the selection criteria, homologs were virtually always positioned on opposite sides of the rosette. Detectable deviations from this precise spatial positioning were often clearly associated with local structural distortions of the rosette, and in many of these instances, visual compensation for obvious structural distortions resulted in the typical homolog distribution pattern.
20. Dual hybridizations with combinations of chromosome-specific alpha-satellite probes and whole-chromosome painting probes were performed on prometaphase chromosome rosettes of HDFs to determine the relative spatial order of chromosomes 7, 8, 16, and X. Hybridization conditions were optimized to facilitate detection of signals emanating from both probes. The spatial order of chromosome homologs was determined by superposition of multiple FISH images representing each dual hybridization over the corresponding phase-contrast image with the use of COREL graphics software.
21. Despite the antiparallel order, the spatial positioning of chromosome homologs was not perfectly symmetrical; comparison of the distribution of chromosome homologs on both sides of the rosette revealed variations in the spatial relations of chromosomes within each half of the rosette (Fig. 3F).
22. T. Freeman and R. Nagele, unpublished observations.
23. We used FISH and centromere-specific DNA probes to investigate spatial and temporal dynamics of centromere topology during the cell cycle in nuclei of HDFs. Before mitosis, centromeric subdomains began to aggregate into discrete centromere chains, each composed of several juxtaposed centromeres. Centromere chains appeared to merge into a single centromere ring that forms the hub of the prometaphase chromosome rosette. These coordinated movements of adjacent centromeric domains provide further indirect evidence that chromosomes may be attached to one another at the level of their centromeres (*22*).
24. HDFs were grown to high density confluence to arrest cells in the G_1 phase of the cell cycle in an effort to minimize cell cycle–dependent variations in chromosome topology. The cell cycle profiles of cultures and individual nuclei were obtained with a CAS 200 Cell Analysis System, which performs a Feulgen-based DNA quantitation. Cells were processed for FISH as described (*12*) with digoxigenin-labeled DNA probes for chromosomes 7, 8, 16, and X (*13*). Chromosomes 7, 8, and 16 were immediately adjacent to chromosome X in 46% (n = 181), 49% (n = 119), and 64% (n = 181) of total nuclei, respectively (*22*). These results support a relation between the spatial positioning of specific chromosomes in the prometaphase rosette and that in the interphase nucleus.
25. HeLa and K562 erythroleukemia cells are both aneuploid, with the number of chromosomes ranging from 65 to 71 in >90% of cells. All chromosomes in these aneuploid cells appeared to be incorporated into a single chromosome rosette at prometaphase.
26. We thank K.-M. Lee and R. Carsia for helpful discussions, and N. Barlow from Micron Optics for help with microscopy.

9 June 1995; accepted 19 September 1995

Diffusion Across the Nuclear Envelope Inhibited by Depletion of the Nuclear Ca^{2+} Store

Lisa Stehno-Bittel,* Carmen Perez-Terzic, David E. Clapham†

Intact, isolated nuclei and a nuclear membrane (ghost) preparation were used to study regulation of the movement of small molecules across the *Xenopus laevis* oocyte nuclear membrane. In contrast to models of the nuclear pore complex, which assume passive bidirectional diffusion of molecules less than 70 kilodaltons, diffusion of intermediate-sized molecules was regulated by the nuclear envelope calcium stores. After depletion of nuclear store calcium by inositol 1,4,5-trisphosphate or calcium chelators, fluorescent molecules conjugated to 10-kilodalton dextran were unable to enter the nucleus. Dye exclusion after calcium store depletion was not dependent on the nuclear matrix because it occurred in nuclear ghosts lacking nucleoplasm. Smaller molecules and ions (500-dalton Lucifer yellow and manganese) diffused freely into the core of the nuclear ghosts and intact nuclei even after calcium store depletion. Thus, depletion of the nuclear calcium store blocks diffusion of intermediate-sized molecules.

Eukaryotic cell nuclei are separated from the cytoplasm by a set of concentric lipid bilayers that form the nuclear envelope. The outer nuclear membrane and lumen of the envelope are continuous with endoplasmic reticulum (*1*). The transport of macromolecules and diffusion of smaller molecules and ions occurs through the nuclear pore complex (*2*), which traverses both nuclear membranes (*3*). Macromolecules greater than 70 kD require adenosine triphosphate (ATP) (*4*) and a nuclear localization sequence (NLS) (*2*, *5*) to be transported. Smaller molecules containing an NLS also require ATP for their transport, but it is thought that there are no regulatory mechanisms for ions and molecules less than 40 to 70 kD that lack an NLS (*6*).

Inositol 1,4,5-trisphosphate ($InsP_3$) releases Ca^{2+} from the nuclear envelope (*7*–*9*). Nuclear $InsP_3$ channels have many of the same characteristics as endoplasmic reticular $InsP_3$ channels (*7*, *8*). Release of intracellular Ca^{2+} blocks transport of intermediate-sized molecules (10 kD) across the nuclear pore in situ (*11*). However, Ca^{2+} release initiates a cascade of events, and thus it is difficult to identify the components responsible for blocking transport across the nuclear envelope in intact cells. To directly assess this question, we developed methods to release Ca^{2+} from the nuclear store and simultaneously measure transport across the nuclear envelope in intact nuclei devoid of nucleoplasm.

Both the nucleoplasm and the lumen of the nuclear envelope (nuclear cisterna) have the potential to regulate Ca^{2+} independently (*12*). Membrane-permeant forms of Ca^{2+}-sensitive dyes load the cisterna preferentially, whereas membrane-impermeant dyes monitor the concentration of Ca^{2+} ($[Ca^{2+}]$) within the nucleoplasm (*10*). To avoid uncertainties when using small mammalian nuclei (2- to 3-μm diameter), we used oocyte nuclei (~500-μm diameter) to visualize the colocalization of the Ca^{2+} store and the nuclear envelope. Nuclei exposed to the membrane-impermeant form of fluo-3 fluoresced throughout the nucleoplasm but not in the region of the nuclear envelope (Fig. 1A). Membrane-permeant fluo-3 (fluo-3 AM) filled the nuclear cisterna as revealed by a thin fluorescent ring (Fig. 1B). The nuclear double membrane itself was defined by the membrane-specific dye rhodamine B (n = 6). No fluorescence was detected in the central region of the nucleoplasm after exposure of the nucleus to fluo-3 AM, as determined by three-dimensional reconstruction of the entire nucleus (n = 3).

Mn^{2+} quenches Ca^{2+}-sensitive dye fluorescence (*10*) and can be used to monitor the flow of ions from the bath into the nuclear cisterna and nucleoplasm. Mn^{2+} (10 μM to 1 mM) rapidly quenched nucleoplasmic fluorescence in nuclei loaded with the membrane-impermeant form of indo-1 (n = 15) (Fig. 1C). In contrast to the rapid equilibration of Mn^{2+} into the nucleoplasm, fluorescence from the nuclear cisterna loaded with indo-1 AM was not altered by the addition of Mn^{2+} even after 30-min exposure to 10 μM Mn^{2+} (n = 5) (Fig. 1D). To monitor Mn^{2+} flux into the nuclear cisterna, we loaded nuclei with both the membrane-permeant and impermeant forms of indo-1 (n = 3). After the addition of Mn^{2+}, fluorescence from the center of the nucleus rapidly dissipated, leaving only the ring structure bounded by

Department of Pharmacology, Mayo Foundation, Rochester, MN 55905, USA.

*Present address: University of Kansas Medical Center, 3901 Rainbow Boulevard, Kansas City, KS 66160–7601, USA.
†To whom correspondence should be addressed.

the nuclear envelope. In the presence of Mn^{2+}, the addition of 1 μM $InsP_3$ resulted in a rapid and complete quench of the fluorescent ring of the nuclear cisterna (Fig. 1D). Thus, activation of $InsP_3$ receptors on the nuclear membrane allowed Mn^{2+} to enter the lumen of the envelope and quench the compartmentalized dye, providing evidence that isolated nuclei are surrounded by an $InsP_3$-sensitive Ca^{2+} store.

Because Mn^{2+} is a trace element, it may not reflect the movement of common cations across the envelope. We measured $[Ca^{2+}]$ in the nucleoplasm using indo-1 while changing $[Ca^{2+}]$ in isotonic or hyperosmotic external solutions. Increasing the external solution osmolarity with mannitol (290 to 690 mosM) had no measurable effects on $[Ca^{2+}]$ in the nucleoplasm or cisterna (n = 23). Increasing bath $[Ca^{2+}]$ from 200 to 500 nM resulted in a rapid increase in nucleoplasmic $[Ca^{2+}]$ without a measurable time delay (n = 15). The nucleoplasmic $[Ca^{2+}]$ followed the extranuclear $[Ca^{2+}]$ linearly up to 1500 nM. Higher $[Ca^{2+}]$ resulted in the loss of integrity of the nuclear envelope and saturation of the dye. In contrast, fluorescence in the nuclear cisterna did not follow changes in external $[Ca^{2+}]$ within the range of 10 nM to 2 μM Ca^{2+} (n = 15). These results suggest that divalent cations (Mn^{2+} and Ca^{2+}) crossed the nuclear envelope and entered the nucleoplasm without significant diffusional barriers.

Fluorescent-bound dextrans of 70 to 500 kD (calcium green) did not diffuse into the *Xenopus* oocyte nucleoplasm (nuclear/bath fluorescence = 0.38 ± 0.02, n = 46) (*13*). However, calcium green conjugated to 10-kD dextran passed into intact, isolated nuclei when added to the bath (nuclear/bath fluorescence = 0.72 ± 0.03, n = 55). To determine whether the nuclear Ca^{2+} store regulated transmembrane diffusion, we exposed intact nuclei to $InsP_3$ (1 μM) for 2 to 5 min to deplete the nuclear Ca^{2+} store and then added the 10-kD form of calcium green to the bath. The dye was excluded from the nucleoplasm in the presence of $InsP_3$ (Fig. 2A) (n = 12). The $InsP_3$ effect resulted from release of Ca^{2+} from the nuclear store because related (control) inositol polyphosphates [Ins(1,3,4)P_3 (1 μM, n = 4) and Ins(1,3,4,5)P_4 (1 μM, n = 5)] that did not release Ca^{2+} at the concentrations we used (*8*) failed to block diffusion of the 10-kD dextran calcium green into the nucleoplasm (Fig. 2B). Depletion of the Ca^{2+} store within the nuclear cisterna by Ca^{2+} chelators blocked subsequent dye entry into the nucleoplasm [10 mM *bis*(2-aminophenoxy) ethane-N,N,N′,N′-tetracetic acid (BAPTA-AM); n = 12] (Fig. 2B). In all experiments, nuclei excluded calcium green bound to 500-kD dextran, indicating that the nuclear envelopes were intact. Thus, depletion of the nuclear Ca^{2+} store by exposure to either $InsP_3$ or BAPTA-AM resulted in block of diffusion of intermediate-sized molecules across the nuclear envelope, eliminating the possibility that local increases in external $[Ca^{2+}]$ caused the block.

When nuclei were incubated in low $[Ca^{2+}]$ (10 nM) for 10 min to deplete the Ca^{2+} store, all nuclei excluded the 10-kD calcium green dye from the nucleoplasm (Fig. 2B) (n = 7). Addition of ATP (1 mM) in the medium containing 10 nM Ca^{2+} did not reverse the effect (Fig. 2B) (n = 7). However, when nuclear cisternal Ca^{2+} stores were repleted by the addition of 2 μM Ca^{2+} plus 1 mM ATP, permeability to 10-kD calcium green dye was restored (Fig. 2B). Because transport of larger molecules (>70 kD) across the nucleus is an ATP-dependent process (*14*), ATP may have actively transported the dye into the nucleus. However, the addition of ATP without Ca^{2+} did not initiate dye movement from the bath into the nuclei (Fig. 2B). Furthermore, energy-dependent transport of large molecules across the nuclear envelope requires an NLS on the transported molecule (*2*, *14*–*16*); NLSs were not present on the substances tested in this study. We conclude that Ca^{2+} and ATP were necessary to replenish the Ca^{2+} supply in the nuclear store but not for transport of the 10-kD molecules themselves.

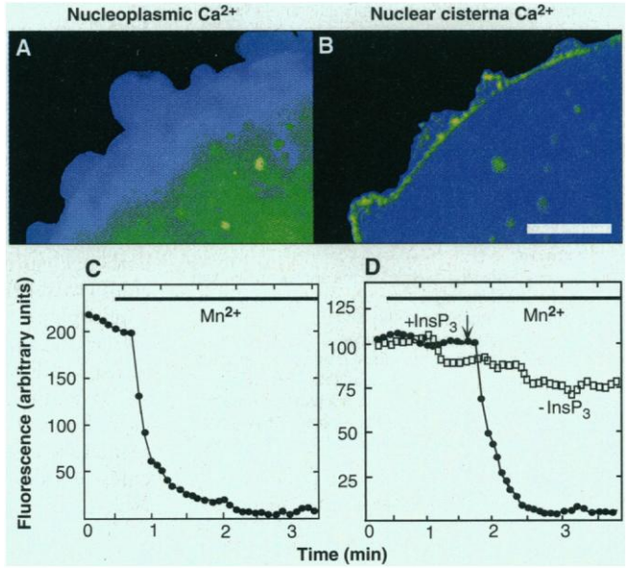

Fig. 1. Differential loading of nuclear compartments. (**A**) Nuclei incubated in membrane-impermeant fluo-3 fluoresced throughout the core of the nucleus. (**B**) Nuclei incubated in membrane-permeant fluo-3 AM fluoresced in a ring consistent with the location of the nuclear envelope. Scale bar, 50 μm; green, high fluorescence levels. (**C**) Mn^{2+} (10 μM) immediately quenched the fluorescence from the nucleoplasm. (**D**) Fluorescence of the nuclear cisterna was much less sensitive to Mn^{2+} (□), but a slow rate of fluorescence decline was observed. Exposure to 1 μM $InsP_3$ caused rapid loss of fluorescence from the cisterna (●).

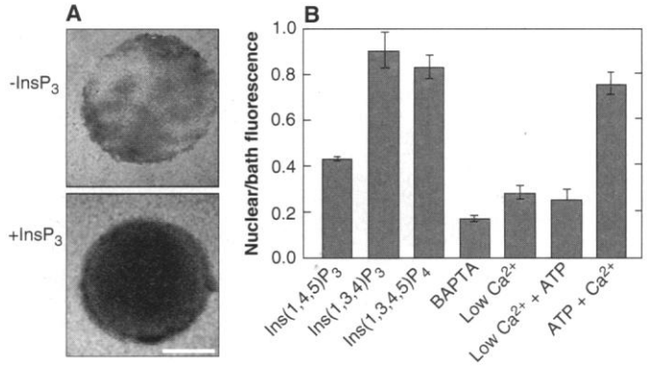

Fig. 2. Exclusion of 10-kD molecules after depletion of the nuclear Ca^{2+} store. (**A**) In the absence of $InsP_3$ (−$InsP_3$), 10-kD fluorescent dyes (calcium green dextran) diffused easily into the nucleoplasm (images taken after 5-min dye exposure). However, after Ca^{2+} store depletion (+$InsP_3$), there was no entry of the 10-kD dextran into the nucleus. Scale bar, 200 μm. (**B**) Exclusion of dye from the nuclei was dependent on depletion of Ca^{2+} from the nuclear store. Agents that depleted the nuclear Ca^{2+} store [Ins(1,4,5)P_3, n = 12; BAPTA-AM, n = 12; and incubation in 10 nM Ca^{2+}, n = 6] also blocked dye diffusion across the nuclear envelope. However, agents that failed to release Ca^{2+} from the nuclear envelope also failed to block dye diffusion [Ins(1,3,4)P_3 or Ins(1,3,4,5)P_4, 1 μM each). After depletion of the nuclear Ca^{2+} store by incubation in 10 nM Ca^{2+} and block of dye influx, ATP was added to the bath. There was no increase in the amount of dye in the nucleus (10 nM Ca^{2+} + low Ca^{2+}/ATP, n = 7). The block of dye diffusion into the nucleus was reversed by the addition of 1 mM ATP + 2 μM Ca^{2+} (ATP + Ca^{2+}).

Because dyes used in these experiments were Ca^{2+}-sensitive, we were concerned that measurement of fluorescence within the nucleus may have resulted from low nucleoplasmic [Ca^{2+}] rather than exclusion of dye. However, depletion of the nuclear Ca^{2+} store also blocked entry of the 10-kD dextran form of the Ca^{2+}-insensitive dye Lucifer yellow into the nucleoplasm (nuclear/bath fluorescence = 0.22 ± 0.03, n = 9). In contrast, when the cisternal Ca^{2+} store was replenished, the nuclear/bath fluorescence increased to 0.78 ± 0.06. These studies confirmed that the nuclear Ca^{2+} store regulates the movement of intermediate-sized molecules (10 kD) across the nuclear envelope.

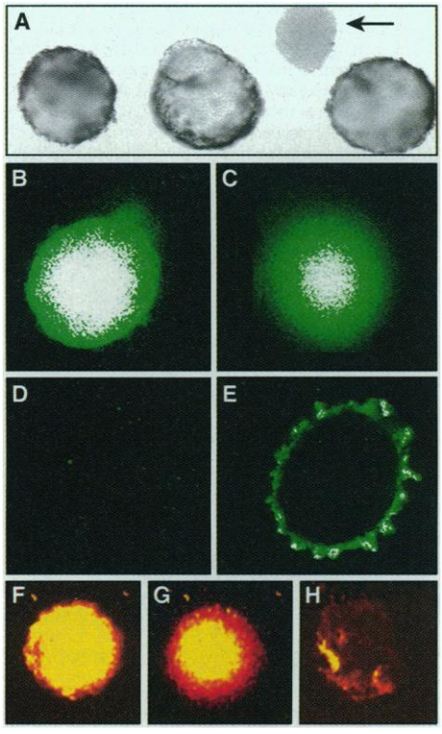

Fig. 3. Separation of nucleoplasmic fluorescence from the intact nuclear envelope in nuclear ghosts. (**A**) Time-elapsed, transmitted light images of a nuclear ghost formed by pricking the nuclear surface. The nucleoplasm was expelled from the nucleus (middle) and the nuclear membrane resealed (right). Arrow indicates the position of the extruded nucleoplasm. (**B**) Loading intact nuclei with the membrane-impermeant form of fluo-3 resulted in fluorescence from the core of the nucleus. During nuclear ghost formation, the nucleoplasm and accompanying fluorescence signal exited the nucleus. (**C**) The extruded nucleoplasm (same nucleus) fluoresced for several minutes. (**D**) The remaining nuclear envelope (ghost) had no fluorescence. (**E**) Subsequent incubation of the same nuclear ghost with fluo-3 AM revealed the ring-like structure of the nuclear envelope. (**F**) An intact nucleus loaded with the chromatin-binding stain, DAPI. (**G**) DAPI-stained nucleoplasm was extruded from the same nucleus. (**H**) The nuclear ghost from the same nucleus retained little fluorescence signal.

Previous studies suggested that the nuclear pore complex does not regulate movement of molecules <70 kD across the nuclear envelope. Gradients of indicator dyes were thought to be artificially created by dye sequestration or exclusion by the nuclear matrix. To determine whether the exclusion of 10-kD calcium green and Lucifer yellow by Ca^{2+} store depletion was a property of the nuclear envelope or the nucleoplasm, we manually separated the two, creating an intact, functional nuclear envelope (nuclear ghost) (*17*) (Fig. 3A). The ghost membranes resealed, leaving an intact nuclear envelope as shown by exclusion of the 500-kD dextran form of calcium green (nuclear/bath fluorescence = 0.07 ± 0.1, n = 7). If the ghost membranes had remained punctured where the nucleoplasm had exited, the 500-kD dye would have readily entered the core of the ghost. Large molecular weight dye exclusion from the core suggested that the nuclear envelope resealed after expulsion of the nucleoplasm.

Separation of the nucleoplasm and the nuclear envelope was tested by loading nuclei with the membrane-impermeant forms of fluo-3 (Fig. 3B) or indo-1. Fluorescence associated with the nucleoplasm was extruded from the nucleus during formation of the nuclear ghost (n = 36). The extruded nucleoplasm fluoresced for >5 min, suggesting that the dye was restricted to the nuclear matrix (Fig. 3C), whereas no fluorescence was detected in the isolated nuclear envelope (Fig. 3D). However, subsequent incubation of the nuclear envelope with the membrane-permeant form of either fluo-3 or indo-1 resulted in fluorescence emission in the region of the nuclear envelope (Fig. 3E). The ring of fluorescence from the ghost nuclear cisterna was not affected by Mn^{2+} in the bath (n = 7), indicating that the inner and outer nuclear membranes had resealed and that cations in the bath did not have access to the dye trapped within the ghost cisterna.

Fluorescence from Ca^{2+}-sensitive dyes in the nucleoplasm during ghost formation may not reflect the amount of endogenous nuclear components, such as chromatin, that accompanied the extruded nucleoplasm. To determine the percentage of nucleotides that remained within the nuclear ghosts, we loaded intact nuclei with either of two DNA-selective stains [Hoechst or 4′,6 diamidine-2-phenylindole (DAPI)] and measured fluorescence during ghost formation (Fig. 3F). Nearly all the fluorescence measured with the DNA stains accompanied the nucleoplasm (Fig. 3G) as compared with the nuclear ghost (Fig. 3H) (n = 6).

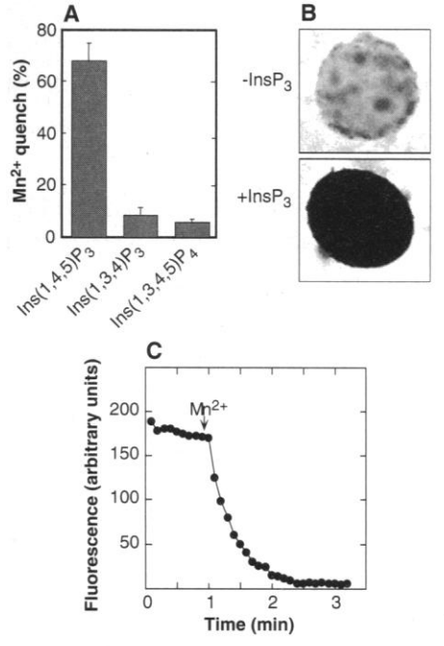

Fig. 4. Ca^{2+} store of nuclear ghosts regulates diffusion of 10-kD molecules across the nuclear envelope. (**A**) Mn^{2+} (10 μM) quenched the indo-1 fluorescence from the nuclear ghost cisterna in the presence of Ins(1,4,5)P_3 (n = 5). In contrast, application of Ins(1,3,4)P_3 or Ins(1,3,4,5)P_4 did not result in Mn^{2+} entry into the cisterna (1 μM, n = 10 each). (**B**) Calcium green dextran (10 kD) entered the nuclear ghosts in the absence of InsP_3 (−InsP_3), but was blocked in the presence of InsP_3 (+InsP_3; nuclear Ca^{2+} store depleted). (**C**) The Ca^{2+}-depleted nuclei permitted Mn^{2+} entry.

To determine whether the Ca^{2+} store within nuclear ghosts was functional and sensitive to InsP_3, we again used Mn^{2+}-induced quench of Ca^{2+}-sensitive dyes. The addition of 1 μM Ins(1,4,5)P_3 to ghosts loaded with indo-1 AM in the presence of Mn^{2+} immediately quenched the signal (n = 5) (Fig. 4A), indicating that the InsP_3 channels had opened and allowed Mn^{2+} to enter the nuclear envelope as observed in the intact nuclei (Fig. 1D). Again, neither Ins(1,3,4)P_3 nor Ins(1,3,4,5)P_4, at the concentrations used, initiated Mn^{2+} entry into the nuclear envelope (n = 10 each) (Fig. 4A). Thus, the inner and outer membrane of nuclear ghosts resealed after ghost formation, and the resulting preparation behaved in a manner similar to that described for intact, isolated nuclei (8).

Ca^{2+} stores of nuclear ghosts also regulated 10-kD molecular diffusion. The 10-kD dye passed quickly into the core of the ghost when the nuclear cisterna was Ca^{2+}-filled by incubation in ATP and Ca^{2+} (average nuclear/bath fluorescence = 0.63 ± 0.06, n = 7) (Fig. 4B). When InsP_3 depleted this store, calcium green was again excluded from the nuclear ghost (10 min of incuba-

tion in the dye; nuclear/bath fluorescence = 0.35 ± 0.09, n = 5). The addition of $InsP_3$ to extruded nucleoplasm did not change the calcium green fluorescence (n = 3), indicating that the lack of fluorescence from the nucleus after $InsP_3$ application was not caused by a direct interaction between components of the nucleoplasm and $InsP_3$. These results eliminate the possibility that the nuclear matrix was necessary for dye exclusion and suggest that the envelope itself regulates transit of intermediate-sized (10 kD) molecules.

Although intermediate-sized molecules of ~10 kD were excluded by the nuclear envelope when the nuclear cisterna Ca^{2+} store was emptied, smaller molecules were not. Intact nuclei were Ca^{2+}-depleted by incubation in 10 nM Ca^{2+} solution with 1 μM $InsP_3$ for 3 min. Nuclei were exposed to a low molecular weight form of Lucifer yellow (500 daltons). Within 2 min after the addition of Lucifer yellow, nuclei had roughly the same fluorescence intensity as the bath (nuclear/bath = 0.84 ± 0.04, n = 8). To determine whether ions were excluded from nuclei, we loaded intact nuclei with the salt form of indo-1 and the nuclear Ca^{2+} store depleted with $InsP_3$. After depletion of stores, 100 μM Mn^{2+} was added to the bath and the fluorescence within the nucleoplasm was monitored. All fluorescence in the nucleoplasm was quenched with the addition of Mn^{2+}, without regard to the amount of Ca^{2+} within the store. In fact, the rate of quench and final fluorescence values were not statistically different in conditions of Ca^{2+}-filled (Fig. 1C) or Ca^{2+}-depleted nuclear stores (n = 8) (Fig. 4C). Lower [Mn^{2+}] (<1 μM) had similar effects (n = 4). Taken together, the results suggest that the nuclear Ca^{2+} store regulates the movement of molecules of ~10 kD, but not smaller molecules or ions.

Our results demonstrate that the nuclear Ca^{2+} store regulates size-specific entry of molecules into the *Xenopus* oocyte nucleus, including intermediate-sized molecules (10 kD) lacking an NLS that were previously thought to pass freely through the nuclear pore complex. We demonstrated that (i) movement of 10-kD molecules across the nuclear envelope depended on Ca^{2+} within the nuclear cisterna; (ii) depletion of this store was sufficient to halt diffusion across the envelope and did not require the nuclear matrix; and (iii) molecules and ions <500 daltons crossed the nuclear envelope regardless of the state of the nuclear Ca^{2+} store. The mechanism by which store depletion is sensed by the nuclear pore is unknown, but the nuclear pore protein, gp210, contains multiple Ca^{2+}-binding domains predicted to reside within the nuclear cisternae (*11*). Such a molecule might sense depletion of the nuclear cisternal [Ca^{2+}] and initiate conformational changes that block intermediate-sized molecule diffusion into the nucleus.

REFERENCES AND NOTES

1. C. Dingwall and R. Laskey, *Science* **258**, 942 (1992); C. Dingwall, *BioEssays* **13**, 213 (1991).
2. L. Davis, *Curr. Opin. Cell Biol.* **4**, 424 (1992).
3. C. W. Akey, *J. Cell Biol.* **109**, 955 (1989).
4. E. C. Hurt, *FEBS Lett.* **325**, 76 (1993).
5. M. S. Moore and G. Blobel, *Cell* **69**, 939 (1992); M. Stewart, *Cell Biol.* **3**, 267 (1992); M. A. Powers and D. J. Forbes, *Cell* **79**, 931 (1994).
6. I. Lang, M. Scholz, R. Peters, *J. Cell Biol.* **102**, 1183 (1986); L. Gerace and B. Burke, *Annu. Rev. Cell Biol.* **4**, 335 (1988); P. A. Silver, *Cell* **64**, 489 (1991).
7. L. Stehno-Bittel, A. Luckhoff, D. E. Clapham, *Neuron* **14**, 163 (1995).
8. D. O. Mak and J. K. Foskett, *J. Biol. Chem.* **269**, 29375 (1994).
9. P. Nicotera, S. Orrenius, T. Nilsson, P. O. Berggren, *Proc. Natl. Acad. Sci. U.S.A.* **87**, 6868 (1990); A. N. Malviya , P. Rogue, G. Vincendon, *ibid.*, p. 9270.
10. G. Grynkiewicz, M. Poenie, R. Y. Tsien, *J. Biol. Chem.* **260**, 3440 (1985); T. J. Hallam and T. J. Rink, *FEBS Lett.* **186**, 175 (1985); C. Lin, G. Hajnoczky, A. P. Thomas, *Cell Calcium* **16**, 247 (1994).
11. U. F. Greber and L. Gerace, *J. Cell Biol.* **128**, 5 (1995).
12. O. Bachs and N. C. E. Agell, *Biochim. Biophys. Acta* **1113**, 259 (1992).
13. *Xenopus laevis* oocytes were removed from toads as described [J. D. Lechleiter and D. E. Clapham, *Cell* **69**, 283 (1992)]. The salt form of fluorescent dyes was injected (50 nl of 1.0 mM dye/oocyte) into oocytes. After 30 min, defolliculated oocytes were enucleated manually by bisecting the oocyte along its equator. Nuclei were removed and washed of cytoplasm in mock intracellular solution containing 140 mM KCl, 10 mM Hepes, 3 mM $MgCl_2$ (pH 7.2). Loading of the nuclear cisterna with membrane-permeant fluorescent dyes was accomplished by incubating the isolated nucleus in mock intracellular solution containing the 100 μM AM form of dye for 15 to 30 min. All fluorescent molecules were purchased from Molecular Probes (Eugene, OR). Nuclei were imaged on a Bio-Rad confocal microscope as described (*8*) or on a Zeiss LSM-410 Laser Scanning confocal microscope. The light source was an argon/krypton laser tuned to either 360 or 488 nm. Two-dimensional confocal images were acquired by scanning 256 by 256 pixels per image. The effective thickness of the confocal optical section was controlled by varying the opening of a pinhole aperture in the detection path. Images were taken every 2 to 5 s, depending on the protocol, with a gray scale value for fluorescence intensity from 1 to 255. Images were processed on a Silicon Graphics Iris computer with ANALYZE software (Mayo Foundation). Background fluorescence values were subtracted in pseudocolor images (Figs. 1 and 3); black represents 0 and blue represents ~1 to 35 arbitrary pixel intensity units. Pixel values were averaged from within the nucleus and divided by the average pixel value of the bath. A ratio value of 1 indicated that fluorescence was equivalent in the nucleus and the bath. Results were expressed as means ± SEM. All experiments were done at room temperature (22° ± 2°C).
14. Nuclear ghosts were formed most commonly by positioning a small air bubble at the end of a micropipette and placing it in contact with the surface of isolated nuclei. Other methods included manually removing the nucleoplasm with a glass micropipette used for microinjection of mammalian cells. Typically, the nucleoplasm required 10 to 15 min to completely exit the nuclear envelope.
15. G. Schlenstedt, E. Hurt, V. Doye, P. A. Silver, *J. Cell Biol.* **123**, 785 (1993).
16. P. L. Paine, M. E. Johnson, Y. T. Lau, L. J. M. Tluczek, D. S. Miller, *BioTechniques* **13**, 238 (1992).
17. M. S. Schmidt-Zachmann, C. Dargemont, L. C. Kuhn, E. A. Nigg, *Cell* **74**, 493 (1993).

18. Supported by NIH grant 41303 to D.E.C.

10 July 1995; accepted 18 October 1995

A Nucleic Acid Triple Helix Formed by a Peptide Nucleic Acid–DNA Complex

Laurie Betts, John A. Josey,* James M. Veal, Steven R. Jordan

The crystal structure of a nucleic acid triplex reveals a helix, designated P-form, that differs from previously reported nucleic acid structures. The triplex consists of one polypurine DNA strand complexed to a polypyrimidine hairpin peptide nucleic acid (PNA) and was successfully designed to promote Watson-Crick and Hoogsteen base pairing. The P-form helix is underwound, with a base tilt similar to B-form DNA. The bases are displaced from the helix axis even more than in A-form DNA. Hydrogen bonds between the DNA backbone and the Hoogsteen PNA backbone explain the observation that polypyrimidine PNA sequences form highly stable 2:1 PNA-DNA complexes. This structure expands the number of known stable helical forms that nucleic acids can adopt.

Oligonucleotides and modified derivatives, such as phosphorothioates, are being examined as antisense therapeutic agents. An ideal antisense agent would be nuclease-resistant and uncharged to aid cellular penetration. A dramatic deviation from the phosphoribose backbone is PNA, originally developed to be an antigene triplexing agent (*1*). PNA is uncharged and stable toward nucleases, and the achiral PNA backbone (Fig. 1A) can be synthesized by amide-based chemistry.

The first report on PNA demonstrated that a T_{10} PNA polymer bound its complementary A_{10} DNA sequence with a markedly increased T_m (temperature at which 50% of double-stranded DNA is

Glaxo Wellcome, 5 Moore Drive, Research Triangle Park, NC 27709, USA.

*Present address: Amgen Boulder, 3200 Walnut Street, Boulder, CO 80301, USA.